

NUMERICAL SOLUTION OF SINGULAR INTEGRAL EQUATIONS IN STRESS CONCENTRATION PROBLEMS

NAO-AKI NODA† and TADATOSHI MATSUO‡

† Department of Mechanical Engineering, Kyushu Institute of Technology, Kitakyushu,
Japan, 804

‡ Department of Mechanical Engineering, Fukushima National College of Technology, Iwaki,
Japan, 970

(Received 8 November 1995; in revised form 16 July 1996)

Abstract—In this paper, the numerical solution of singular integral equations in stress concentration problems is considered. The idea of the body force method stress field induced by a point force in an infinite body is used as a fundamental solution. Then, the problem is formulated as an integral equation with a singularity of the form of r^{-1} . In solving the integral equations, the boundary conditions satisfied by two types of numerical procedure are examined. Then, it is found that the unknown functions of body force densities should be approximated by the product of a polynomial and several types of fundamental density functions. The calculation shows that this latter method gives a smooth variation of stresses along the elliptical boundary for various geometrical and loading conditions. In addition, this method gives rapidly converging numerical results and highly satisfied boundary conditions along the entire boundary. © 1997 Elsevier Science Ltd.

NOTATION

a :	major radius of elliptical hole
b :	minor radius of elliptical hole
(x, y) :	rectangular coordinate
(ξ, η) :	(x, y) coordinate where point force is applied
θ :	eccentric angle of ellipse
ϕ :	eccentric angle of ellipse for the point (ξ, η)

1. INTRODUCTION

As a result of computer developments, various numerical methods useful for stress analysis have been developed. Among those methods, singular integral equation method has been applied to many crack problems (Erdogan and Gupta, 1972; Erdogan *et al.*, 1973; Sih, 1973; Theocaris and Ioakimidis, 1977; Boiko and Kerpenko, 1981; Erdogan, 1983a, b; Kaya and Erdogan, 1987; Fujimoto, 1990; Noda and Matsuo, 1991). In the analysis, a crack is represented by a distribution of infinitesimal dislocations in a plate without a crack. Then, the problem is reduced to singular integral equations having Cauchy-type singular kernel. This method, however, has hardly been applied to other than the boundary of the crack, such as hole, notch and inclusions.

On the other hand, the body force method, which was originally proposed by Nisitani (Nisitani, 1967, 1974; Nisitani and Chen, 1987), has been applied to various stress concentration problems. In solving the two dimensional notch problems, the body force method uses the stress field of a point force in an infinite plate as a fundamental solution. In the numerical solution, the concept of the fundamental density function was originally proposed, and the unknown function of the body force density was approximated by the products of “fundamental density functions” and “weight functions”. Here, the fundamental density function is an exact density of body force to express a single elliptical hole exactly. The weight function is chosen to be a “step function”, which takes a constant value along each segment into which a whole boundary is discretized; each constant value

of the step function is determined from the boundary condition at the mid-point of each segment (Nisitani, 1967, 1974; Nisitani and Chen, 1987).

In the previous papers, the numerical solutions of the singular integral equation of the body force method in 2D crack problems have been discussed (Noda *et al.*, 1989, 1990, 1991, 1992, 1993; Noda and Oda, 1992). In those papers, unknown functions of the body force densities have been approximated by using polynomials instead of the step functions. It has been found that a new method gives the results of better accuracy with shorter CPU time compared with the conventional body force method using the step functions.

Initially, in this paper, the singular integral equation of the body force method is shown in the analysis of stress concentration problem. Then, the numerical solution of the conventional body force method is discussed by applying two types of numerical procedure. In the former method "A", the known weight functions are approximated as continuous functions by using polynomials instead of step functions. The results show that method A has better convergence rate than the conventional body force method; however, it is found that this former method cannot completely satisfy the boundary condition along the boundaries. On the other hand, in method "B", eight kinds of fundamental density functions are newly defined and applied. The results show that introducing the new fundamental functions can satisfy the boundary conditions along the entire boundary. It is found that this latter method yields a smooth variation of stresses along the boundary with higher accuracy compared with other methods.

In this paper, some simple problems are taken as examples of stress concentration problems in order to explain the numerical solutions and results. However, the numerical method developed here can be applied to various stress concentration problems and especially suited for elliptical boundaries; for example, arbitrarily distributed elliptical holes (Noda and Matsuo, 1995a, b), elliptical inclusions (Noda and Matsuo, 1996a, b), and a row of semi-elliptical notches (Noda *et al.*, 1996). The idea of the use of several types of "fundamental densities" may be applied to other than the boundary of ellipse.

2. NUMERICAL SOLUTION OF SINGULAR INTEGRAL EQUATION OF THE CONVENTIONAL BODY FORCE METHOD (METHOD A)

2.1. Numerical solution using the singular integral equation of conventional body force method

Consider an infinite plate under uniform tension having two elliptical holes as shown in Fig. 1. Here, an infinite plate with two elliptical holes [$x = \pm(d + a \cos \theta)$, $y = b \sin \theta$] subjected to tension is taken as a sample problem to explain the numerical solution. The problem can be formulated in terms of singular integral equation by using a Green's function: that is, the stress field at an arbitrary point (x, y) when point forces act symmetrically on another two points $(\pm \xi, \eta)$ in an infinite plate. The formation is based simply on the principle of the superposition. Here, (ξ, η) is a point in the (x, y) coordinate system where point forces are applied. Based on the body force method, the problem is reduced to determining the density of body force, that is, embedded point forces in an infinite plate, along the prospective boundary of the holes in the infinite plate without holes.

$$\begin{aligned}
 & - (1/2) \{ \rho_x^*(\theta) \cos \theta_0 + \rho_y^*(\theta) \sin \theta_0 \} + \int_{\Gamma} K_{mn}^{Fx}(\phi, \theta) \rho_x^*(\phi) ds \\
 & + \int_{\Gamma} K_{mn}^{Fy}(\phi, \theta) \rho_y^*(\phi) ds = - (\sigma_x^{\infty} \cos^2 \theta_0 + \sigma_y^{\infty} \sin^2 \theta_0) \\
 & - (1/2) \{ -\rho_x^*(\theta) \sin \theta_0 + \rho_y^*(\theta) \cos \theta_0 \} + \int_{\Gamma} K_{ni}^{Fx}(\phi, \theta) \rho_x^*(\phi) ds \\
 & + \int_{\Gamma} K_{ni}^{Fy}(\phi, \theta) \rho_y^*(\phi) ds = - (\sigma_y^{\infty} - \sigma_x^{\infty}) \sin \theta_0 \cos \theta_0 \quad (1)
 \end{aligned}$$

where

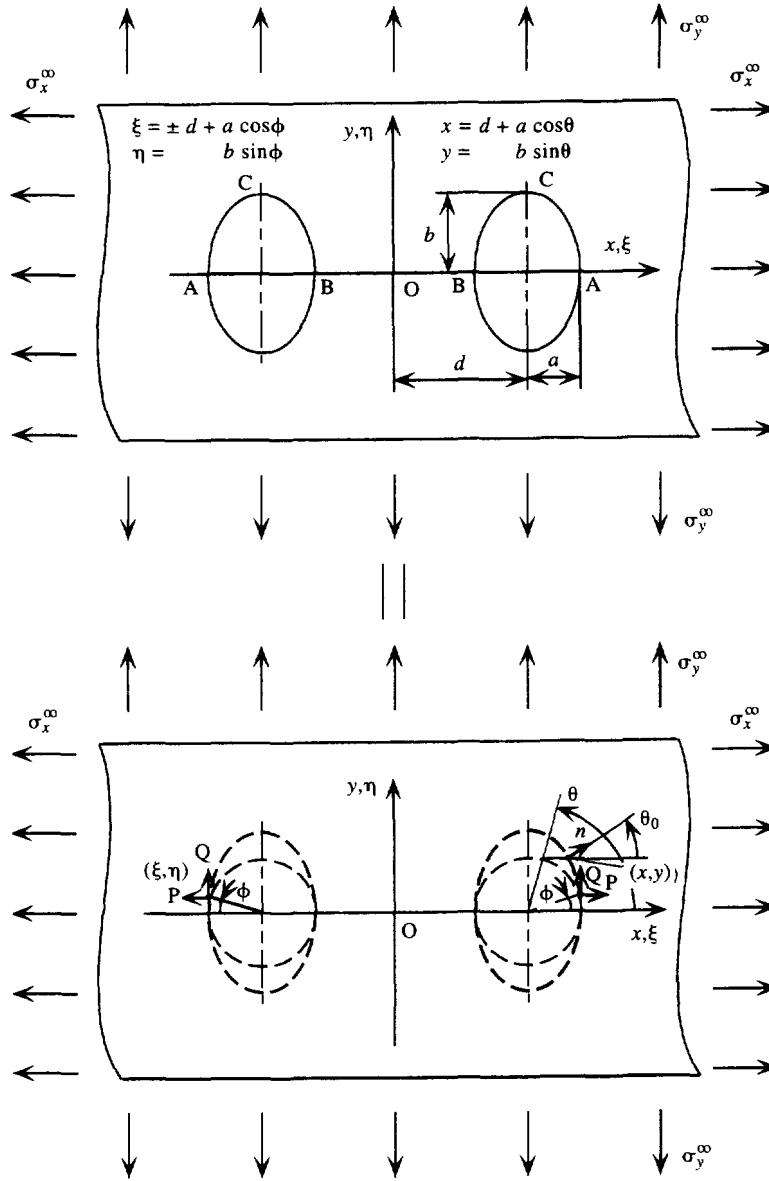


Fig. 1. Two circular holes in an infinite plate under tension.

$$-d\xi = a \sin \phi d\phi, \quad d\eta = b \cos \phi d\phi, \quad ds = \sqrt{a^2 \sin^2 \phi + b^2 \cos^2 \phi} d\phi, \quad \tan \theta_0 = (a/b) \tan \theta.$$

Here, Γ denotes the boundary for an elliptical boundary and θ_0 is the angle between the x -axis and the normal direction at the point (x, y) on the ellipse. In eqn (1), the unknown functions are the body force densities $[\rho_x^*(\phi), \rho_y^*(\phi)]$ distributed along the prospective boundaries in the x, y -directions. Here, ϕ is the angle that specifies the points where body forces are distributed. Equations (1) are the boundary conditions at the imaginary boundary; that is, $\sigma_n = 0$ and $\tau_m = 0$. It should be noted that the body forces lie within the prospective cavities. The first terms of eqns (1) represent the stress due to the body force distributed on the "minus boundary" (Nisitani, 1967). The "minus boundary" means the imaginary boundary composed of the internal points that are an infinitesimally small distance from the initial boundary. Taking $K_m^{Ex}(\phi, \theta)$ for example, the notation means the normal stress σ_n induced at the point when the body forces with unit density in the x -direction is acting symmetrically to the y -axis along the infinitesimal arc length on the elliptical boundary. These equations include the singular terms having the singularity of

the form $1/\{\sin(\theta-\phi)/2\}$ (Nisitani and Chen, 1987). In this case, $\theta = \phi$, the integration should be interpreted as the meaning of Cauchy's principle values.

In the conventional body force method, the unknown functions in eqns (1) $\rho_x^*(\phi)$, $\rho_y^*(\phi)$ are expressed by the following equations,

$$\begin{aligned}\rho_x^*(\phi) &= \frac{dF_\xi}{ds} = \frac{dF_\xi}{d\eta} n_x(\phi) = \rho_x(\phi) n_x(\phi), \\ \rho_y^*(\phi) &= \frac{dF_\eta}{ds} = -\frac{dF_\eta}{d\xi} n_y(\phi) = \rho_y(\phi) n_y(\phi),\end{aligned}\quad (2)$$

where dF_ξ , dF_η are the components of the resultant of the body force in the x , y directions acting on an infinitesimal arc length ds , respectively. Here, $n_x(\phi)$, $n_y(\phi)$ are the x , y components $[= (\cos \theta_0, \sin \theta_0)]$ of the normal unit vector, respectively, at the point (x, y) . They are expressed by the following equations.

$$n_x(\phi) = \frac{b \cos \phi}{\sqrt{a^2 \sin^2 \phi + b^2 \cos^2 \phi}}, \quad n_y(\phi) = \frac{a \sin \phi}{\sqrt{a^2 \sin^2 \phi + b^2 \cos^2 \phi}}, \quad (3)$$

where $\rho_x(\phi)$, $\rho_y(\phi)$ are the body force densities of the unit projected length in the x , y directions (Nisitani, 1967, 1974; Nisitani and Chen, 1987).

$$\rho_x(\phi) = \frac{dF_\xi}{d\eta}, \quad \rho_y(\phi) = -\frac{dF_\eta}{d\xi}. \quad (4)$$

Using the expression of eqns (4), the singular integral eqns (1) become the following equations,

$$\begin{aligned}- (1/2) \{ \rho_x(\phi) \cos^2 \theta_0 + \rho_y(\phi) \sin^2 \theta_0 \} + \int_0^{2\pi} K_{mn}^{Fx}(\phi, \theta) \rho_x(\phi) b \cos \phi \, d\phi \\ + \int_0^{2\pi} K_{mn}^{Fy}(\phi, \theta) \rho_y(\phi) a \sin \phi \, d\phi = -(\sigma_x^\infty \cos^2 \theta_0 + \sigma_y^\infty \sin^2 \theta_0) \\ - (1/2) \{ -\rho_x(\theta) + \rho_y(\theta) \} \sin \theta_0 \cos \theta_0 + \int_0^{2\pi} K_{ni}^{Fx}(\phi, \theta) \rho_x(\phi) b \cos \phi \, d\phi \\ + \int_0^{2\pi} K_{ni}^{Fy}(\phi, \theta) \rho_y(\phi) a \sin \phi \, d\phi = -(\sigma_y^\infty - \sigma_x^\infty) \sin \theta_0 \cos \theta_0 \quad (0 \leq \theta \leq \pi). \quad (5)\end{aligned}$$

It should be noted that $n_x(\phi)$, $n_y(\phi)$ are regarded as a kind of "fundamental densities" to approximate $\rho_x^*(\phi)$, $\rho_y^*(\phi)$ very accurately. They are actually the exact densities of the body forces for the problem of an isolated elliptical hole in an infinite plate under tension (Nisitani, 1967, 1974; Nisitani and Chen, 1987). In the conventional body force method, the elliptical boundary is divided into small segments, then the unknown weighting functions $\rho_x(\phi)$, $\rho_y(\phi)$ have been approximated by step functions, which take a constant value along each segment. While in method A, polynomials have been applied to approximate the unknown functions as continuous function. Now, from the symmetry of the problem, the following expression can be used,

$$\begin{aligned}\rho_x(\phi) &= \sum_{n=1}^{M/2} a_n t_n(\phi) \quad (-\pi/2 \leq \theta \leq \pi/2) \\ t_n(\phi) &= \cos((\pi/2 - \phi)(n-1)) \quad (1 \leq n \leq M/2)\end{aligned}$$

$$\rho_x(\phi) = \sum_{n=M/2+1}^M a_n s_n(\phi) \quad (\pi/2 \leq \theta \leq 3\pi/2)$$

$$s_n(\phi) = \cos((\pi/2 - \phi)(n - M/2 - 1)) \quad (M/2 + 1 \leq n \leq M) \tag{6}$$

$$\rho_y(\phi) = \sum_{n=1}^M b_n t_n(\phi)$$

$$t_n(\phi) = \cos((\pi/2 - \phi)(n - 1)). \tag{7}$$

In preliminary studies using the conventional body force method, it has been found that the weight function $\rho_x(\phi)$ is discontinuous at $\theta = \pm \pi/2$; therefore, as shown in eqn (6), $\rho_x(\phi)$ is expressed individually in the two ranges $-\pi/2 \leq \theta \leq \pi/2$ and $\pi/2 \leq \theta \leq 3\pi/2$. Using the approximation method mentioned above, we obtain the following system of linear equations for the determination of the coefficients a_n, b_n, c_n, d_n . The number of unknown coefficients is $2M$. The collocation points are set as given in eqn (8) to the determination of the coefficients.

$$\theta_L = \frac{\pi}{M}(L - 0.5) \quad 1 \leq L \leq M \tag{8}$$

$$\sum_{n=1}^M (a_n A_n + b_n B_n) = -(\sigma_x^\infty \cos^2 \theta_0 + \sigma_y^\infty \sin^2 \theta_0)$$

$$\sum_{n=1}^M (a_n C_n + b_n D_n) = -(\sigma_y^\infty - \sigma_x^\infty) \sin \theta_0 \cos \theta_0 \tag{9}$$

$$A_n = -(1/2)s_n(\theta) \cos^2 \theta_0 + \int_{-\pi/2}^{\pi/2} K_{nn}^{Fx}(\phi, \theta) b \cos \phi s_n(\phi) d\phi \quad (1 \leq n \leq M/2)$$

$$A_n = -(1/2)s_n(\theta) \cos^2 \theta_0 + \int_{\pi/2}^{3\pi/2} K_{nn}^{Fx}(\phi, \theta) b \cos \phi s_n(\phi) d\phi \quad (M/2 + 1 \leq n \leq M)$$

$$B_n = -(1/2)t_n(\theta) \sin^2 \theta_0 + \int_0^{2\pi} K_{nn}^{Fy}(\phi, \theta) a \sin \phi t_n(\phi) d\phi$$

$$C_n = (1/2)t_n(\theta) \sin \theta_0 \cos \theta_0 + \int_{-\pi/2}^{\pi/2} K_{nn}^{Fx}(\phi, \theta) b \cos \phi t_n(\phi) d\phi \quad (1 \leq n \leq M/2)$$

$$C_n = (1/2)t_n(\theta) \sin \theta_0 \cos \theta_0 + \int_{\pi/2}^{3\pi/2} K_{nn}^{Fx}(\phi, \theta) b \cos \phi t_n(\phi) d\phi \quad (M/2 + 1 \leq n \leq M)$$

$$D_n = -(1/2)t_n(\theta) \sin \theta_0 \cos \theta_0 + \int_0^{2\pi} K_{nn}^{Fy}(\phi, \theta) a \sin \phi t_n(\phi) d\phi. \tag{10}$$

For collocation points, evenly spaced intervals of the θ_L have been used in both analysis methods A and B as shown in eqns (8) and (17). On the other hand, in crack problems, it is well-known that setting more collocation points near crack tips is advantageous in generating high accuracy of the results. Some other sets of collocation points of eqn (8) have also been tried and they are found to cause insignificant difference from the present results.

Table 1. Convergence of maximum stress by method A ($\sigma_x^\infty = 0, \sigma_y^\infty = 1$)

(a) $a/b = 1 \quad d/a = 3$					
M	Present analysis		M	B.F.M.	
	K_{iA}	K_{iB}		K_{iA}	K_{iB}
4	3.02246	2.99350	4	3.01615	3.00564
8	3.02018	2.99247	8	3.01823	2.99917
12	3.02000	2.99246	16	3.01921	2.99571
16	3.02001	2.99240	32	3.01967	2.99395
			48	3.01982	2.99336
			∞ (48-32)	3.0201	2.9922
			Ling	3.020	2.992

(b) $a/b = 2 \quad d/a = 3$					
M	Present analysis		M	B.F.M.	
	K_{iA}	K_{iB}		K_{iA}	K_{iB}
4	5.04461	5.04732	4	5.04264	5.05363
8	5.04493	5.04717	8	5.04383	5.05035
12	5.04485	5.04719	16	5.04440	5.04868
16	5.04486	5.04716	32	5.04467	5.04785
			48	5.04475	5.04758
			∞ (48-32)	5.0449	5.0470

Table 2. Convergence of maximum stress by method A ($\sigma_x^\infty = 1, \sigma_y^\infty = 0$)

$a/b = 1 \quad d/a = 3$				
M	Present analysis		M	B.F.M.
	K_i			K_i
4	2.82543		4	2.82074
8	2.82456		8	2.82273
12	2.82432		16	2.82386
16	2.82455		32	2.82445
			48	2.82464
			∞ (48-32)	2.82503
			Ling	2.825

2.2. Numerical results using the singular integral equation of conventional body force method

Table 1 shows the convergence of stresses at points A and B when $a/b = 1, d/a = 3, \sigma_x^\infty = 0, \sigma_y^\infty = 1$ (Table 1(a)) and when $a/b = 2, d/a = 3, \sigma_x^\infty = 0, \sigma_y^\infty = 1$ (Table 1(b)) with increasing collocation number, in comparison with the conventional body force method using step-function to approximate the unknown function $\rho_x(\phi), \rho_y(\phi)$. Table 2 also shows the convergence of stresses at point C when $a/b = 1, d/a = 3, \sigma_x^\infty = 1, \sigma_y^\infty = 0$. The results of Ling (1948) are shown in Tables 1 and 2. These tables indicate that the present analysis has a better convergence rate than the conventional body force method. In order to investigate how accurately the boundary conditions are satisfied ($\sigma_n = 0, \tau_{nt} = 0$), boundary stresses $\sigma_n, \sigma_t, \tau_{nt}$ along the hole when the collocation number $M = 16$ have been indicated as shown in Tables 3 and 4. These tables show that the boundary conditions are not satisfied very well, especially around the point C. It should be noted that the residual stresses are skew-symmetrically distributed with respect to the point C.

The reason why the boundary conditions cannot be satisfied completely is as follows. In both method A and the conventional body force method, only the fundamental density functions $n_x(\phi), n_y(\phi)$, namely, the exact densities of the body forces for an isolated elliptical hole have been used. They are symmetrical to the point C, and, in addition, since $n_x(\phi)$ approaches zero when ϕ approaches $\pm \pi/2$, the body force $\rho_x^*(\phi)$ also approaches zero and, therefore, the residual shear stresses cannot be satisfied in the solution shown by eqns (2)-(10).

Table 3. Compliance of the boundary condition by method A
($\sigma_x^c = 0, \sigma_y^c = 1$)

θ (deg.)	$a/b = 1, d/a = 3, M = 16$		
	σ_t	σ_n	τ_{nt}
0	3.02001	-0.000317	0.000000
20	2.55390	-0.000333	-0.000345
40	1.37677	-0.000139	-0.000179
60	0.04621	0.000788	0.001175
80	-0.80503	0.002580	0.009009
86	-0.88051	-0.000609	-0.006905
88	-0.90409	-0.000093	-0.013961
90	-0.91981	0.000000	-0.015511
92	-0.92579	0.000093	-0.013961
94	-0.92017	0.000609	-0.006905
100	-0.79335	-0.002580	0.009009
120	0.10783	-0.000788	0.001175
140	1.43530	0.000139	-0.000179
160	2.56053	0.000333	-0.000345
180	2.99240	0.000370	0.000000

Table 4. Compliance of the boundary condition by method A
($\sigma_x^c = 1, \sigma_y^c = 0$)

θ (deg.)	$a/b = 1, d/a = 3, M = 16$		
	σ_t	σ_n	τ_{nt}
0	-0.33660	0.000646	0.000000
20	-0.04927	0.000666	0.000691
40	0.81904	0.000278	0.000358
60	1.96456	-0.001577	-0.002349
80	2.72493	-0.005158	0.018011
86	2.72493	0.001219	0.013805
88	2.79911	-0.001865	0.027910
90	2.82455	0.000000	0.031079
92	2.83067	0.001865	0.027910
94	2.79846	-0.001219	0.013805
100	2.70069	0.005158	0.018011
120	1.85017	0.001577	-0.002349
140	0.72476	-0.000278	0.000358
160	-0.06917	-0.000666	0.000691
180	-0.32415	-0.000640	0.000000

3. NEW SOLUTION OF SINGULAR INTEGRAL EQUATION OF THE BODY FORCE METHOD (METHOD B)

3.1. Definition of new fundamental density functions

New fundamental density functions for the body forces in the x -direction $w_x(\phi)$ and the ones in the y -direction $w_y(\phi)$ are defined by the following expression (Noda and Matsuo, 1992, 1993, 1995).

$$\begin{aligned}
 w_{x1}(\phi) &= n_x(\phi) / \cos \phi \\
 w_{x2}(\phi) &= n_x(\phi) \tan \phi \\
 w_{x3}(\phi) &= n_x(\phi) \\
 w_{x4}(\phi) &= n_x(\phi) \sin \phi \\
 w_{y1}(\phi) &= n_y(\phi) / \sin \phi \\
 w_{y2}(\phi) &= n_y(\phi) \\
 w_{y3}(\phi) &= n_y(\phi) \cot \phi \\
 w_{y4}(\phi) &= n_y(\phi) \cos \phi.
 \end{aligned}
 \tag{11}$$

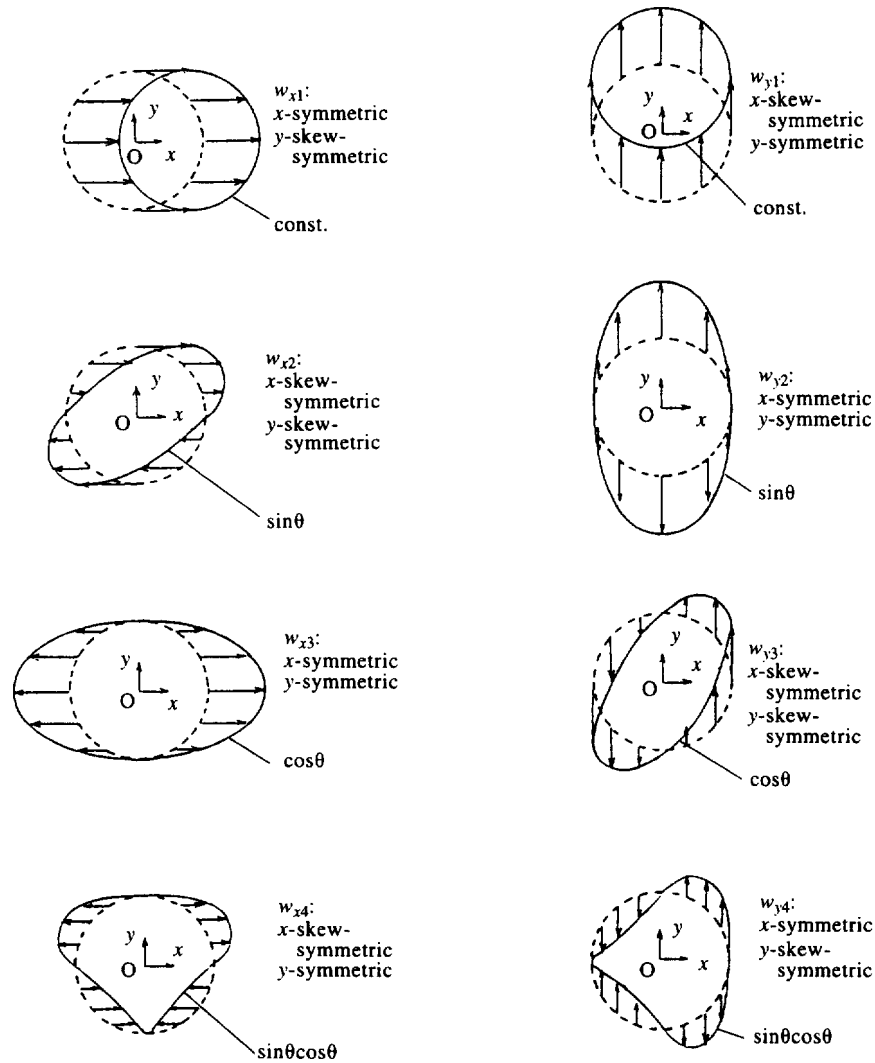


Fig. 2. New fundamental density functions for circular boundary.

The fundamental density functions defined by eqn (11) are shown in Fig. 2 for a circular boundary.

The unknown functions of the body force densities for elliptical holes $\rho_x^*(\phi)$, $\rho_y^*(\phi)$ can be expressed by a linear combination of the fundamental density functions defined by eqns (11) and the weight functions $\rho_{x1}(\phi)$, $\rho_{x2}(\phi)$, ..., $\rho_{y4}(\phi)$, as shown in the following equations.

$$\begin{aligned} \rho_x^*(\phi) &= \rho_{x1}(\phi)w_{x1}(\phi) + \rho_{x2}(\phi)w_{x2}(\phi) + \rho_{x3}(\phi)w_{x3}(\phi) + \rho_{x4}(\phi)w_{x4}(\phi) \\ \rho_y^*(\phi) &= \rho_{y1}(\phi)w_{y1}(\phi) + \rho_{y2}(\phi)w_{y2}(\phi) + \rho_{y3}(\phi)w_{y3}(\phi) + \rho_{y4}(\phi)w_{y4}(\phi) \end{aligned} \quad (12)$$

Using the eqns (12), $\rho_x^*(\phi)$, $\rho_y^*(\phi)$ which are defined over $0 \leq \phi \leq 2\pi$, can be expressed by the weight functions $\rho_{x1}(\phi)$, $\rho_{x2}(\phi)$, ..., $\rho_{y4}(\phi)$. These weight functions are symmetric with respect to the axes $\phi = 0, \pi/2, \pi, 3\pi/2$.

$$\begin{aligned} \rho_x^*(\phi) &= \rho_{x1}(\phi)w_{x1}(\phi) + \rho_{x3}(\phi)w_{x3}(\phi) \\ \rho_y^*(\phi) &= \rho_{y2}(\phi)w_{y2}(\phi) + \rho_{y4}(\phi)w_{y4}(\phi) \end{aligned} \quad (13)$$

3.2. New solution of the singular integral equation of the body force method

Using the expressions in eqns (11)–(13), the singular integral eqn (1) is reduced to the following eqns (14) instead of eqn (5)

$$\begin{aligned}
 & - (1/2)[\{\rho_{x1}(\theta)/\cos\theta + \rho_{x3}(\theta)\} \cos^2\theta_0 + \{\rho_{y2}(\theta) + \rho_{y4}(\theta)\cos\theta\} \sin^2\theta_0] \\
 & \quad + \int_0^{2\pi} K_{mn}^{Fx}(\phi, \theta) \{\rho_{x1}(\phi)/\cos\phi + \rho_{x3}(\phi)\} b \cos\phi \, d\phi \\
 & + \int_0^{2\pi} K_{mn}^{Fy}(\phi, \theta) \{\rho_{y2}(\phi) + \rho_{y4}(\phi)\cos\phi\} a \sin\phi \, d\phi = -(\sigma_x^\infty \cos^2\theta_0 + \sigma_y^\infty \sin^2\theta_0) \\
 & - (1/2)[-\{\rho_{x1}(\theta)/\cos\theta + \rho_{x3}(\theta)\} + \{\rho_{y2}(\theta) + \rho_{y4}(\theta)\cos\theta\}] \sin\theta_0 \cos\theta_0 \\
 & \quad + \int_0^{2\pi} K_{ni}^{Fx}(\phi, \theta) \{\rho_{x1}(\phi)/\cos\phi + \rho_{x3}(\phi)\} b \cos\phi \, d\phi \\
 & + \int_0^{2\pi} K_{ni}^{Fy}(\phi, \theta) \{\rho_{y2}(\phi) + \rho_{y4}(\phi)\cos\phi\} a \sin\phi \, d\phi = -(\sigma_y^\infty - \sigma_x^\infty) \sin\theta_0 \cos\theta_0. \quad (14)
 \end{aligned}$$

In the present analysis, polynomials have been used to approximate the unknown functions as continuous function. Now, from the symmetry of the problem, the following expression can be applied.

$$\begin{aligned}
 \rho_{x1} &= \sum_{n=1}^{M/2} a_n t_n(\phi), & \rho_{y2} &= \sum_{n=1}^{M/2} b_n t_n(\phi) \\
 \rho_{x3} &= \sum_{n=1}^{M/2} c_n t_n(\phi), & \rho_{y4} &= \sum_{n=1}^{M/2} d_n t_n(\phi)
 \end{aligned} \quad (15)$$

$$t_n(\phi) = \cos\{2(n-1)\phi\}. \quad (16)$$

Using the approximation method mentioned above, we obtain the following system of linear equations for the determination of the coefficients a_n, b_n, c_n, d_n . The number of unknown coefficients is $2M$. The collocation points are set as given by eqn (17).

$$\theta_L = \frac{\pi}{M}(L-0.5) \quad 1 \leq L \leq M \quad (17)$$

$$\begin{aligned}
 \sum_{n=1}^{M/2} (a_n A_n + b_n B_n + c_n C_n + d_n D_n) &= -(\sigma_x^\infty \cos^2\theta_0 + \sigma_y^\infty \sin^2\theta_0) \\
 \sum_{n=1}^{M/2} (a_n E_n + b_n F_n + c_n G_n + d_n H_n) &= -(\sigma_y^\infty - \sigma_x^\infty) \sin\theta_0 \cos\theta_0
 \end{aligned} \quad (18)$$

$$A_n = - (1/2)t_n(\theta) \cos^2\theta_0 / \cos\theta + \int_0^{2\pi} K_{nn}^{Fx}(\phi, \theta) t_n(\phi) b \, d\phi$$

$$B_n = - (1/2)t_n(\theta) \cos^2\theta_0 + \int_0^{2\pi} K_{nn}^{Fy}(\phi, \theta) t_n(\phi) b \cos\phi \, d\phi$$

$$C_n = - (1/2)t_n(\theta) \sin^2\theta_0 + \int_0^{2\pi} K_{nn}^{Fx}(\phi, \theta) t_n(\phi) a \sin\phi \, d\phi$$

$$D_n = - (1/2)t_n(\theta) \sin^2\theta_0 \cos\theta + \int_0^{2\pi} K_{nn}^{Fy}(\phi, \theta) t_n(\phi) a \sin\phi \cos\phi \, d\phi$$

Table 5. Convergence of unknown functions by method B ($\sigma_x^\infty = 0, \sigma_y^\infty = 1$)

θ (deg.)	M	$a/b = 1, a/d = 1/3$			
		ρ_{x_3}	ρ_{y_2}	ρ_x	ρ_{y_4}
0	4	-0.8914	2.9828	-0.0301	0.0528
	8	-0.8899	2.9787	-0.0401	0.0615
	12	-0.8899	2.9787	-0.0401	0.0615
20	4	-0.8972	2.9875	-0.0276	0.0517
	8	-0.8971	2.9853	-0.0282	0.0579
	12	-0.8971	2.9853	-0.0282	0.0579
40	4	-0.9120	2.9994	-0.0062	0.0489
	8	-0.9135	3.0000	-0.0026	0.0498
	12	-0.9135	3.0000	-0.0026	0.0498
60	4	-0.9288	3.0129	0.0180	0.0457
	8	-0.9288	3.0137	0.0197	0.0419
	12	-0.9288	3.0137	0.0197	0.0419
80	4	-0.9398	3.0217	0.0338	0.0436
	8	-0.9373	3.0211	0.0312	0.0375
	12	-0.9373	3.0211	0.0312	0.0375
90	4	-0.9413	3.0229	0.0360	0.0433
	8	-0.9384	3.0221	0.0326	0.0370
	12	-0.9384	3.0221	0.0326	0.0369

$$\begin{aligned}
 E_n &= -(1/2)t_n(\theta) \sin \theta_0 \cos \theta_0 / \cos \theta + \int_0^{2\pi} K_{nt}^{Fx}(\phi, \theta) t_n(\phi) b d\phi \\
 F_n &= -(1/2)t_n(\theta) \sin \theta_0 \cos \theta_0 + \int_0^{2\pi} K_{nt}^{Fy}(\phi, \theta) t_n(\phi) b \cos \phi d\phi \\
 G_n &= -(1/2)t_n(\theta) \sin \theta_0 \cos \theta_0 + \int_0^{2\pi} K_{nt}^{Fy}(\phi, \theta) t_n(\phi) a \sin \phi d\phi \\
 H_n &= -(1/2)t_n(\theta) \sin \theta_0 \cos \theta_0 \cos \theta + \int_0^{2\pi} K_{nt}^{Fy}(\phi, \theta) t_n(\phi) a \sin \phi \cos \phi d\phi. \quad (19)
 \end{aligned}$$

The stresses at an arbitrary point are represented by a linear combination of the coefficients a_n, b_n, c_n, d_n and the influence coefficients corresponding to A_n, B_n, \dots, H_n .

Using the numerical solution mentioned above, we will obtain the stress concentration factors and the stress distribution along the boundaries.

3.3. Numerical results using the new solution of singular integral equation of the body force method

Tables 5 and 6 show the convergence of unknown functions $\rho_{x3}(\phi), \rho_{y2}(\phi), \rho_{x1}(\phi), \rho_{y4}(\phi)$ along the prospective boundary of circular hole with increasing the collocation number. The present results have the convergency to the fourth digit when $M = 8$. Figures 3 and 4 show the variation of the unknown functions in comparison with the results of conventional body force method, where only two unknown functions $\rho_x(\phi), \rho_y(\phi)$ are approximated by using the stepped functions when $M = 12, 24$. In the present results four unknown functions of the body force densities, $\rho_{x3}(\phi), \rho_{y2}(\phi), \rho_{x1}(\phi), \rho_{y4}(\phi)$ seem to approximate the continuous density distributions very well because the present results of $M = 8$ and $M = 12$ coincide with each other to the fifth digits. On the other hand, two unknown functions $\rho_x(\phi), \rho_y(\phi)$ do not converge with an increasing number of collocation points as shown in Figs 3 and 4. The reason is that $\rho_x(\phi), \rho_y(\phi)$ cannot represent the actual

Table 6. Convergence of unknown functions by method B ($\sigma_x^\infty = 1, \sigma_y^\infty = 0$)

θ (deg.)	M	$b/a = 1, a/d = 1/3$			
		ρ_{x_1}	ρ_{y_2}	ρ_{x_3}	ρ_{y_4}
0	4	2.7796	-0.8476	0.0704	-0.1267
	8	2.7776	-0.8419	0.0764	-0.1394
	12	2.7776	-0.8419	0.0764	-0.1394
20	4	2.7894	-0.8564	0.0539	-0.1247
	8	2.7893	-0.8534	0.0548	-0.1338
	12	2.7893	-0.8534	0.0548	-0.1338
40	4	2.8140	-0.8786	0.0122	-0.1196
	8	2.8160	-0.8796	0.0068	-0.1209
	12	2.8160	-0.8796	0.0068	-0.1209
60	4	2.8420	-0.9038	0.0352	-0.1138
	8	2.8418	-0.9050	-0.0377	-0.1081
	12	2.8418	-0.9050	-0.0377	-0.1082
80	4	2.8603	-0.9203	-0.0661	-0.1100
	8	2.8565	-0.9194	-0.0621	-0.1008
	12	2.8565	-0.9194	-0.0621	-0.1008
90	4	2.8628	-0.9226	-0.0704	-0.1095
	8	2.8584	-0.9212	-0.0652	-0.0998
	12	2.8584	-0.9212	-0.0652	-0.0998

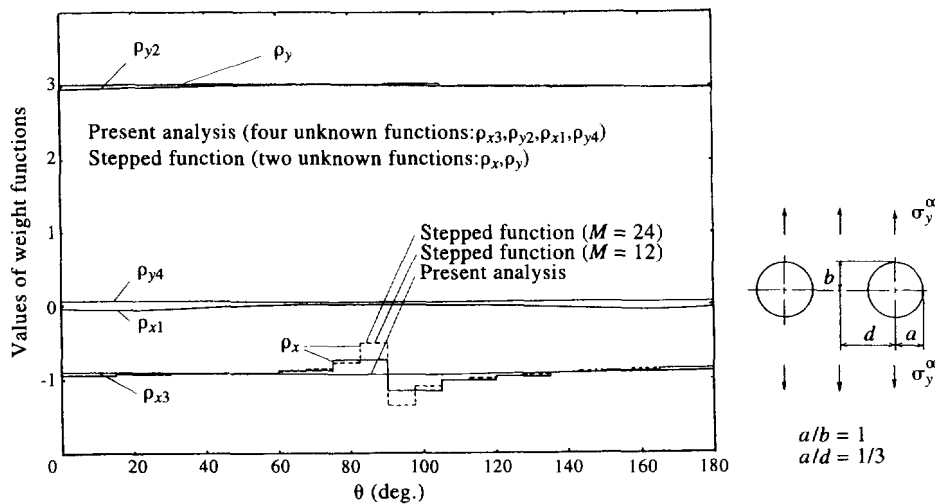


Fig. 3. Variation of unknown functions by method B in comparison with the conventional body force method ($\sigma_x^\infty = 0, \sigma_y^\infty = 1$).

density distribution $\rho_x^*(\phi), \rho_y^*(\phi)$ enough, especially near $\theta = \pi/2$, because of the fundamental density functions $n_x(\phi), n_y(\phi)$ approaches zero when $\theta = \pi/2$.

To investigate the satisfaction of the boundary conditions ($\sigma_n = 0, \tau_{nt} = 0$), the stresses $\sigma_n, \sigma_t, \tau_{nt}$ along the elliptical boundary have been investigated as shown in Tables 7 and 8. The values of σ_n, τ_{nt} which should be 0 along the boundary are less than 10^{-5} , even when $M = 8$. In the present analysis, therefore, the boundary requirements can be highly satisfied along the entire boundary by the use of new fundamental functions.

As another example, two ellipsoidal cavities in an infinite body under tension as shown in Fig. 5 is solved in a similar way using another Green's function, that is, the stress field at an arbitrary point (r, z) when ring forces act symmetrically on another two points $(\pm \rho, \zeta)$ in an infinite body (Nisitani and Noda, 1984). Table 9 shows the results of stress σ_θ at points A and B in comparison with the results of Tsuchida *et al.* (1976) when $a/b = 1, \sigma_x^\infty = 1, \sigma_z^\infty = 0$. The method B yields rapidly converging numerical results for the wide range of a/d . The present results and Tsuchida's results coincide with each other to the

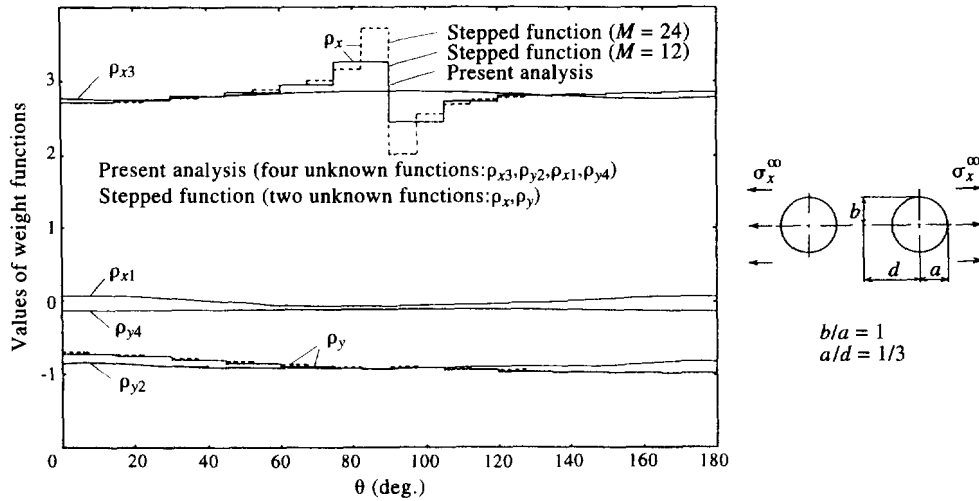


Fig. 4. Variation of unknown functions by method B in comparison with the conventional body force method ($\sigma_r^\infty = 1, \sigma_z^\infty = 0$).

Table 7. Compliance of the boundary condition by method B ($\sigma_r^\infty = 1, \sigma_z^\infty = 0$)

θ (deg.)	M	$a/b = 1, a/d = 1/3$		τ_{nr}
		σ_r	σ_n	
0	4	3.0188	-9.4×10^{-4}	0
	8	3.0197	-2.9×10^{-6}	0
	12	3.0197	-4.9×10^{-9}	0
40	4	1.3759	8.1×10^{-4}	-5.0×10^{-4}
	8	1.3747	-2.0×10^{-6}	1.2×10^{-4}
	12	1.3747	2.1×10^{-9}	-1.3×10^{-9}
80	4	-0.8154	-3.7×10^{-4}	8.7×10^{-4}
	8	-0.8135	-2.4×10^{-7}	5.6×10^{-7}
	12	-0.8135	1.1×10^{-9}	-2.7×10^{-9}
90	4	-0.9191	-3.1×10^{-4}	1.2×10^{-3}
	8	-0.9188	-8.6×10^{-7}	3.7×10^{-6}
	12	-0.9188	-1.3×10^{-9}	6.0×10^{-9}
100	4	-0.7812	-7.3×10^{-5}	1.0×10^{-3}
	8	-0.7829	-3.7×10^{-8}	7.0×10^{-7}
	12	-0.7829	1.5×10^{-10}	-3.2×10^{-9}
140	4	1.4358	-1.1×10^{-3}	-1.3×10^{-3}
	8	1.4379	2.4×10^{-6}	2.8×10^{-6}
	12	1.4379	-2.5×10^{-9}	-2.9×10^{-9}
180	4	2.9929	2.0×10^{-3}	0
	8	2.9908	5.4×10^{-6}	0
	12	2.9908	8.5×10^{-9}	0

third significant digit. The results when $a/b = 1, \sigma_r^\infty = 0, \sigma_z^\infty = 1$ was shown in the previous paper (Noda and Matsuo, 1995). The magnitude and position of maximum stress of two ellipsoidal cavities under tension are shown in Table 10 ($\sigma_r^\infty = 0, \sigma_z^\infty = 1$) and Table 11 ($\sigma_r^\infty = 1, \sigma_z^\infty = 0$) for various values of a/b .

4. CONCLUSION

In this paper, singular integral equations of the body force method were formulated by using the stress field of a point force as a fundamental solution. Then, then numerical solution was considered in the analysis of stress concentration problems.

Table 8. Compliance of the boundary conditions by method B ($\sigma_x^z = 1, \sigma_y^z = 0$)

θ (deg.)	M	$b/a = 1, a/d = 1/3$		
		σ_t	σ_n	τ_{nt}
0	4	-0.9376	-1.4×10^{-3}	0
	8	-0.9391	3.7×10^{-6}	0
	12	-0.9391	5.8×10^{-9}	0
40	4	0.6548	-1.2×10^{-3}	7.7×10^{-4}
	8	0.6567	2.5×10^{-6}	-1.6×10^{-6}
	12	0.6567	-2.5×10^{-9}	1.6×10^{-9}
80	4	2.7413	5.9×10^{-4}	1.3×10^{-3}
	8	2.7385	3.1×10^{-7}	-7.3×10^{-7}
	12	2.7384	-1.3×10^{-9}	3.2×10^{-9}
86	4	2.8190	5.9×10^{-4}	-1.7×10^{-3}
	8	2.8174	1.1×10^{-6}	3.8×10^{-6}
	12	2.8174	1.3×10^{-9}	-4.6×10^{-9}
88.6	4	2.8264	5.4×10^{-4}	-1.8×10^{-3}
	8	2.8255	1.1×10^{-6}	-4.5×10^{-6}
	12	2.8255	1.7×10^{-9}	-6.7×10^{-9}
90	4	2.8233	5.0×10^{-4}	-1.9×10^{-3}
	8	2.8228	1.1×10^{-6}	4.7×10^{-6}
	12	2.8228	1.6×10^{-9}	-7.1×10^{-9}
94	4	2.7910	3.6×10^{-4}	-1.9×10^{-3}
	8	2.7917	6.8×10^{-7}	-4.1×10^{-6}
	12	2.7917	7.7×10^{-10}	-4.9×10^{-8}
100	4	2.6735	1.3×10^{-4}	-1.6×10^{-3}
	8	2.6761	5.1×10^{-8}	-8.8×10^{-7}
	12	2.6761	-1.9×10^{-10}	3.8×10^{-9}
140	4	0.5597	1.6×10^{-3}	1.9×10^{-3}
	8	0.5567	-3.0×10^{-6}	-3.5×10^{-6}
	12	0.5567	3.0×10^{-9}	3.4×10^{-9}
180	4	-0.8381	-3.0×10^{-3}	0
	8	-0.8350	-6.7×10^{-6}	0
	12	-0.8350	-1.0×10^{-8}	0

In the conventional body force method, the unknown functions of the body force densities has been approximated by the products of the fundamental density functions and weight functions. Here:

- (a) the fundamental density function is an exact density of body force to express a single elliptical hole; and
- (b) the weight function is chosen to be a "step function", which takes a constant value along each segment into which a whole boundary is discretized.

In this paper, to solve the integral equations accurately, the boundary conditions satisfied by two types of numerical procedure (methods A and B) are examined. The conclusions are summarized as follows:

- (1) In the former method A, the known weight functions were approximated as continuous functions by using polynomials instead of step functions. The results show that method A has better convergence rate than the conventional body force method. However, it was found that this former method cannot completely satisfy the boundary condition along the boundaries. The reason is that the conventional fundamental density functions cannot represent real density distribution enough near the apex of elliptical boundary.
- (2) In the later method B, eight kinds of fundamental density functions were newly defined and applied; then, the unknown functions of the body force densities were approximated by a linear combination of the new fundamental density functions and weight functions.

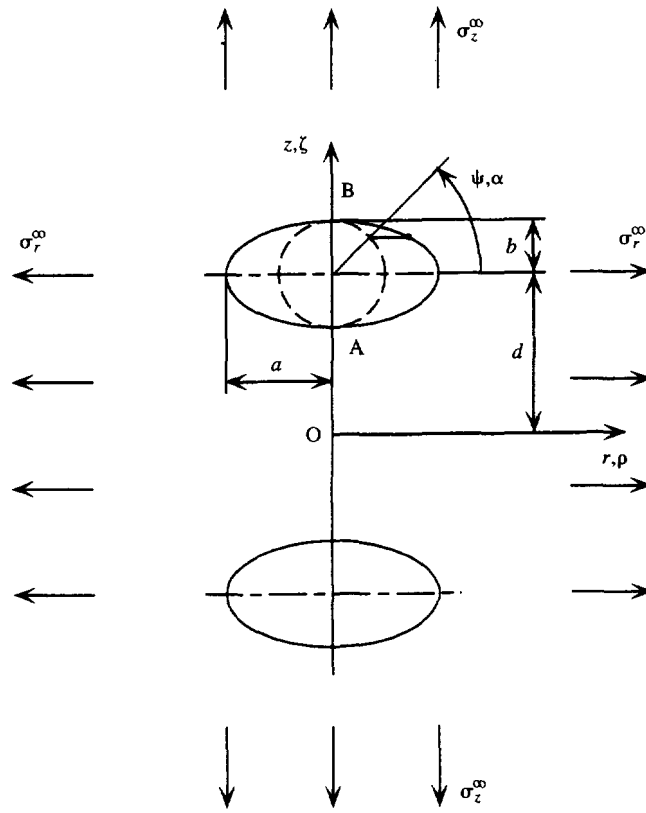


Fig. 5. Two ellipsoidal cavities in an infinite body subjected to σ_r^∞ and σ_z^∞ .

Table 9. Results of two spherical cavities in an infinite body under tension ($a/b = 1, \sigma_r^\infty = 1, \sigma_z^\infty = 0$)

a/d	A ($\psi = -90^\circ$)		B ($\psi = 90^\circ$)	
	Present analysis	Tsuchida	Present analysis	Tsuchida
0	2.1820	2.182	2.1820	2.182
0.1	2.1817	2.18	2.1818	2.18
0.2	2.1798	2.18	2.1812	2.18
0.3	2.1730	2.17	2.1803	2.18
0.4	2.1572	2.16	2.1795	2.18
0.5	2.1292	2.13	2.1796	2.18
0.6	2.0954	2.09	2.1809	2.18
0.7	2.0939	2.09	2.1840	2.19
0.8	2.2395	2.24	2.1889	2.19
0.9	2.8130		2.1960	

Table 10. Results of two ellipsoidal cavities in an infinite body under tension ($\sigma_r^\infty = 0, \sigma_z^\infty = 1$)

b/d a/b	0	1/3		1/2		2/3	
	K_0	ψ (deg.)	K_1	ψ (deg.)	K_1	ψ (deg.)	K_1
1/2	1.4403	0.2	1.4365	0.7	1.4285	2.0	1.4159
1	2.0455	0.3	2.0200	1.2	1.9800	2.4	1.9394
2	3.3130	0.6	3.1515	1.5	3.0269	2.1	2.9492
4	5.8678	0.6	5.1063	1.2	4.9734	1.5	4.8634
8	10.9706	0.5	8.9554	0.8	8.6904	0.8	8.5604

The results show that introducing the new fundamental functions can satisfy the boundary conditions along the entire boundary. It is found that this latter method yields a smooth variation of stresses along the boundary with higher accuracy compared with other methods.

Table 11. Results of two ellipsoidal cavities in an infinite body under tension ($\sigma_x^\infty = 1, \sigma_z^\infty = 0$)

b/d a/b	0		1/3		1/2		2/3	
	$K_{I,0}$	ψ (deg.)	K_I	ψ (deg.)	K_I	ψ (deg.)	K_I	ψ (deg.)
1	2.1819	90.0	2.1799	90.0	2.1795	90.0	2.1827	
1/2	2.5373	90.0	2.5369	90.0	2.5366	90.0	2.5368	
1/4	2.7404	-90.0	2.7409	-90.0	2.7449	-90.0	2.7611	
1/8	2.8221	90.0	2.8210	90.0	2.8213	90.0	2.8214	

(3) As an example, the interaction of two ellipsoidal cavities in an infinite body is analyzed. The results of two spheroidal cavities coincide with Tsuchida's results to the third significant digit. The exact stress concentration factors are indicated in tables with varying the shape and space. It is found that the method B yields rapidly converging numerical results for the wide geometrical range.

REFERENCES

- Boiko, A. V. and Karpenko, L. N. (1981). On some numerical methods for the solution of the plane elasticity problem for bodies with cracks by means of singular integral equations. *International Journal of Fracture* **17**, 381–388.
- Erdogan, F. (1983a). Stress intensity factors. *ASME Journal of Applied Mechanics* **25**, 992–1002.
- Erdogan, F. (1983b). Mixed boundary value problems in mechanics. *Mechanics Today* **4**, 1–86.
- Erdogan, F. and Gupta, G. D. (1972). On the numerical solution of singular integral equations. *Quarterly Applied Mathematics* **30**, 525–534.
- Erdogan, F., Gupta, G. D. and Cook, T. S. (1973). Numerical solution of singular integral equations. In *Mechanics of Fracture* (ed. Sih, G. C.) Noordhoff International Publication, Leyden, pp. 368–425.
- Fujimoto, K. (1990). Method of numerical analysis of the singular integral equations for crack analysis. *Transactions of the Japanese Society of Mechanical Engineers* (in Japanese) **56**, 1050–1510.
- Kaya, A. C. and Erdogan, F. (1987). On the solution of integral equations with strongly singular kernels. *Quarterly Applied Mathematics* **45**, 105–122.
- Ling, C. B. (1948). On the stresses in a plate containing two circular holes. *Journal of Applied Physics* **19**, 77–82.
- Nisitani, H. (1967). The two-dimensional stress problem solved using an electric digital computer. *Journal of the Japanese Society of Mechanical Engineers* **70**, 627–632.
- Nisitani, H. (1974). Solution of notch problems by body force method. In *Stress Analysis of Notched Problem* (ed. Sih, G. C.), Noordhoff International Publication, Leyden, pp. 1–68.
- Nisitani, H. and Chen, D. H. (1987). *Body Force Method* (Taiseikiryokuho in Japanese) Baihukan.
- Nisitani, H. and Noda, N. A. (1984). Stress concentration of a cylindrical bar with a v-shaped circumferential groove under torsion, tension or bending. *Engineering Fracture Mechanics* **20**, 743–766.
- Noda, N. A. and Matsuo, T. (1991). Numerical solution of singular integral equations using polynomial expansion method. *Transactions of the Japanese Society of Mechanical Engineers* (in Japanese) **57**, 2811–2816.
- Noda, N. A., Umeki, H. and Erdogan, F. (1989). Singular integral equation method in the analysis of a crack perpendicular to the interface. *Transactions of the Japanese Society of Mechanical Engineers* (in Japanese) **55**, 2521–2526.
- Noda, N. A., Oda, K. and Chen, D. H. (1990). Hypersingular integral equation method in the analysis of mixed mode crack problems. *Transactions of the Japanese Society of Mechanical Engineers* (in Japanese) **56**, 2405–2410.
- Noda, N. A., Oda, K. and Masuda, C. (1991). Hypersingular integral equation method in the analysis of kinked and branched cracks. *Transactions of the Japanese Society of Mechanical Engineers* (in Japanese) **57**, 2332–2337.
- Noda, N. A. and Oda, K. (1992). Numerical solutions of the singular integral equations in the crack problems using the body force method. *International Journal of Fracture* **58**, 285–304.
- Noda, N. A., Oda, K. and Ishii, K. (1993). Analysis of stress intensity factors for curved cracks. *Transactions of the Japanese Society of Mechanical Engineers* (in Japanese) **59**, 332–336.
- Noda, N. A., Oda, K. and Matsuo, T. (1992). Numerical solutions of the singular integral equations of the body force method in notch and crack problems. In *Localized Damage II, Vol. 2: Computational Method in Fracture Mechanics* (eds Adiabadi, M. H., Nisitani, H. and Cartwright, D. J.), Computational Mechanics Publications, Southampton, pp. 35–56.
- Noda, N. A. and Matsuo, T. (1992). Numerical solution of singular integral equations of the body force method in notch problems (first report, basic theory and discussion on the stress along the boundary). *Transactions of the Japanese Society of Mechanical Engineers* (in Japanese) **58**, 2179–2184.
- Noda, N. A. and Matsuo, T. (1993). Numerical solution of singular integral equations of the body force method in notch problems (second report, analysis of interaction problems of notches under general loading conditions). *Transactions of the Japanese Society of Mechanical Engineers* (in Japanese) **55**, 785–791.
- Noda, N. A. and Matsuo, T. (1993). Numerical solution of singular integral equations having cauchy-type singular kernel by means of expansion method. *International Journal of Fracture* **63**, 229–245.
- Noda, N. A. and Matsuo, T. (1995a). Singular integral equation method in the analysis of interaction between cracks and defects. *Fracture Mechanics* **25**, 591–605.

- Noda, N. A. and Matsuo, T. (1995b). Singular integral equation method in optimization of stress relieving hole : a new approach based on the body force method. *International Journal of Fracture* **70**, 147–165.
- Noda, N. A. and Matsuo, T. (1996a). Singular integral equation method for interaction between elliptical inclusions. *Transactions of ASME, Series E, Journal of Applied Mechanics* (submitted).
- Noda, N. A. and Matsuo, T. (1996b). Interaction between elliptical inclusions under a shear stress field. *Transactions of ASME, Series E, Journal of Applied Mechanics* (submitted).
- Noda, N. A., Matsuo, T. and Tsuru, M. (1996). Tension of a semi-infinite plate containing a row of semi-elliptical notches and edge cracks. *Engineering Fracture Mechanics* (submitted).
- Sih, G. C. (ed.) (1973). *Method of Analysis and Solutions of Crack Problems*, Noordhoff International Publication, Leyden.
- Theocaris, P. S. and Ioakimidis, N. I. (1977). Numerical integration method for the solution of singular integral equation. *Quarterly Applied Mathematics* **35**, 173–183.
- Tuchida, E., Nakahara, I. and Kodama, M. (1976). Asymmetric problem of elastic body containing several spherical cavities (first report, elastic body containing two spherical cavities). *Transactions of the Japanese Society of Mechanical Engineers* (in Japanese) **42**, 46–54.